Journal of Advanced Joining Processes 9 (2024) 100225

Contents lists available at ScienceDirect

Journal of Advanced Joining Processes

journal homepage: www.sciencedirect.com/journal/journal-of-advanced-joining-processes

Fatigue behavior of adhesive joints under modes I and II fracture in carbon-epoxy composites, influence of exposure time in a saline environment

P. Vigón [a], A. Argüelles [a], M. Lozano [a], J. Viña [b,*]

[a] Department of Construction and Manufacturing Engineering, University of Oviedo, Edificio Departamental Oeste n 7, Campus de Viesques, 33203, Gijón, Spain
[b] Department of Materials Science and Metallurgical Engineering, University of Oviedo, Edificio Departamental Este, Campus de Viesques, 33203, Gijón, Spain

ARTICLE INFO

Keywords:
Composite
Delamination
Adhesive
Fracture
Fatigue

ABSTRACT

This work investigates the fatigue crack growth behavior of adhesive joints under pure modes I and II within epoxy matrix composites reinforced with unidirectional carbon fibers. Experimental tests are made using Double Cantilever Beam (DCB) and End-Notched Flexure (ENF) setups for modes I and II respectively, considering exposure periods of one week and twelve weeks in a salt spray chamber. Control specimens are also studied for comparison.

Static tests were conducted to securely establish the levels of Energy Release Rate (ERR) that were subsequently used to obtain the fatigue initiation curves (G-N) and fatigue crack growth curves (G-da/dN). A probabilistic model based on a Weibull distribution is applied to analyze fatigue initiation data.

The fatigue limit in mode I, for all aging periods, is around 25 % of the static strength, while in mode II, it is around 20 %. These results are very close at all aging levels (0, 1, and 12 weeks). From this, it is inferred that aging in a saline environment of the studied joints does not have a significant impact on the fatigue limit.

In the crack growth zone, for mode I, the velocity is higher in the specimens aged in both periods than in the unaged specimens. The same cannot be said for mode II, where a clear trend cannot be appreciated.

Introduction

The high specific strength and stiffness of composite make them ideal for use in structures where weight is a crucial factor. However, composite materials fabricated from sheets are susceptible to the occurrence and propagation of cracks between layers. This phenomenon, known as delamination, represents one of the primary failure modes significantly limiting the service life of these materials. Delamination can arise from defects introduced during either the manufacturing process or the component operational lifespan. Failures during service may result from interlaminar stresses induced by applied loading conditions or environmental factors. The combined influence of these factors contributes to the initiation of delamination

Usually, delamination growth results in a reduction of strength and stiffness of the composite, leading to structural failure. This situation, which occurs in the internal layers of a composite plate, also happens when two composite plates are joined using an adhesive. Once again, the ideal conditions are created for the phenomenon of delamination to occur, in this case, with the growth of a crack in the adhesive zone. Brunner et al. (2021) and Desai et al. (2023) compile the different types of failure that can happen in an adhesive joint, while Delzendehroo et al. (2021) include a relationship with existing regulations for fracture characterization, among other aspects, of adhesive joints.

In previous studies of this type of joints, the significant importance of pre-treatment of substrate surfaces has been clearly demonstrated. Yildirim et al. (2023) analyzed the effect of atmospheric plasma treatment on the fracture toughness properties (modes I and II) of adhesively bonded carbon fiber/PEKK composite joints. They discovered that plasma-treated surfaces exhibited an increase in average surface roughness, which enhanced adhesive wettability and the fracture resistance. Martínez-Landeros et al. (2019) conducted various surface treatments, including cleaning, sanding, acid etching, and peel ply, resulting in increased values of inter-laminar fracture toughness for CFRPs. Similar objectives were pursued by Del Real et al. (2011), who employed an acrylic adhesive. In the case of Saleh et al. (2021), they modified the adhesive by including tannic acid in its composition,

* Corresponding author.
E-mail address: jaure@uniovi.es (J. Viña).

https://doi.org/10.1016/j.jajp.2024.100225

Available online 21 April 2024

significantly altering its wettability and mode I fracture toughness in the bonded joints.

In addition, a significant number of studies have been conducted where the fracture behavior of adhesive joints was examined. In the case of mode I fracture, the works of Lima et al. (2022) are focused, comparing the results monitored using optical fiber located within the high strength steel joint with an epoxy adhesive with those obtained by DIC and visual observations, yielding good correlations between the three methods.Mohan et al. (2014) contrast the results obtained for mode I fracture in co-cured and secondary bonded joints. Finally, González Ramírez et al. (2018) analyze fatigue delamination in composite joints. In the case of mode II fracture, Akhavan-Safar et al. (2023) analyzed the effect of low cycle impact fatigue on mode II fracture energy. Clerca et al. (2019) conducted quasi-static and cyclic fatigue fracture mode II tests for adhesive wood joints. Orell et al. (2023) used DIC tool to verify crack growth in mode II, while Zabala et al. (2016), instead of using the ENF test to induce mode II, employed the 4ENF. Even Delzendehroo et al. (2021) questioned whether studying mode II fracture is useful for understanding the behavior of the adhesive joint.

Another parameter whose influence on the joint has been studied in recent years is temperature. In this line of research, there are works on general properties of joints, such as the one by Santos et al. (2023), and many others focused on the impact on fracture and fatigue. For instance, Tan et al. (2021) analyzed the fatigue behavior of a joint made with polyurethane. Fernandes et al. (2016) studied the effect of temperature on modes I and II, while Vikas et al. (2021) solely focused on the influence of cryogenic temperatures on fracture.

Similarly, there are several studies that analyze the influence of the environment on adhesive properties. Vigón et al. (2022) compared the impact of exposure to salt spray and hygrothermal aging on static delamination. In a similar vein, Teixeira de Freitas et al. (2017) investigated the influence of salt spray exposure for up to 90 days on a joint with Steel and CFRP adherents, using the peel test. Argüelles et al. (2022) examined the effect of exposure to a saline environment on dynamic fracture behavior in mode I. Other studies focus on analyzing the influence of water and humidity. For instance, Almandour et al. (Almansour et al., 2017) studied the water absorption effect on mode I fracture toughness of flax/basalt reinforced vinylester composites, observing distinct behavior during initiation and propagation. Johar et al. (2019) conducted a similar investigation for various fracture modes using a carbon/epoxy composite immersed at 70 °C for different periods.

Brito et al. (2020) studied the combined effect of humidity and temperature (hygrothermally aged) on the adhesive joint tested under mode I loading at -54 °C, 25 °C, and 80 °C, detecting a significant modification in the ERR (Energy Release Rate). Similarly, Katafiasz et al. (2021) observed the same phenomenon in the mode I fracture test of CFRPs toughened with thermoplastic particles, which were tested after moisture saturation at -55 °C, 19 °C, and 90 °C. Lastly, a significant group of authors focused on analyzing the influence of environmental conditions on the properties of the joint. In this context, the work by Sousa et al. (2023) investigated single lap joints made of duplex stainless steel. The results revealed that both temperature and humidity significantly reduced the fatigue strength of the joints, particularly for shorter fatigue lives, by up to 10 times. Abdel-Monsef et al. (2021) studied mode II fracture, conducting tests at high and low temperatures. Their wet-aged specimens were exposed to accelerated aging in an environmental chamber at 70 °C/85 % RH for four years.

The aim of this study was to evaluate how adhesive joints perform in resisting delamination fatigue when exposed to varying durations in a saline environment. For this purpose, a composite material consisting of an epoxy matrix and unidirectional carbon fiber reinforcement was select, with an epoxy-based adhesive chosen as the bonding agent. For the characterization of the joint resistance to delamination, the ERR reached by the joint under mode I and mode II of fracture stress was taken as a study parameter. The influence of exposure periods to a saline environment on adhesive joints and their impact on fatigue life were analyzed, considering both the initiation and the crack growth for each fracture mode.

Materials

The description below includes the materials used in this study, encompassing both the composite material used as substrate, as well as the type of adhesive employed.

The specimens had the following dimensions: a width of 20 mm and a length of 150 mm, with a crack initiation length of 60 mm from the sample end. The total thickness of each specimen was 4.3 ± 0.1 mm. Additionally, a 12 μm thick polytetrafluoroethylene (PTFE) anti-adhesive film was placed between the substrates at one end, as an initiator for the delamination process, as show in Fig. 1.

Composite material

The composite material used in this work, as substrate, is composed of an epoxy matrix and unidirectional carbon fiber reinforcement with commercial designation MTC510-UD300-HS-33 %RW manufactured by SHD Composites. The mechanical properties of the laminate are experimentally obtained in accordance with standards and are presented in Table 1.

The laminate was manufactured using vacuum molding and the reinforcing fibers were positioned in a unidirectional orientation at 0°. Then, two layers of the laminate will be bonded using the selected adhesive.

The thermal curing cyclerecommended by the manufacturer was applied. During the first hour of the curing cycle, the temperature is rised progressively from ambient temperature to 100 °C. It is maintained at this temperature for three and a half hours, and then it is increased from 100 °C to 120 °C with a velocity of 40 °C per hour. This temperature is maintained for another hour. When the temperature cycle finished, the material continues in the oven until it returns to ambient temperature.

Surface treatment

The composite material used as the substrate was surface-conditioned by manually sanding with Al_2O_3 sandpaper with a grit size of P220. After treating the surface of the composite, it was cleaned and degreased, and then the bonding process was carried out.

Properties of the adhesive

A commercial epoxy-based adhesive, Loctite® EA 9461TM, was used to bond each of the two parts of the final laminate, whose surfaces were pre-treated. The properties of the adhesive are shown in Table 2. Then, the curing cycle recommended by the manufacturer was applied. It consists of a pressure of 4 bars and a temperature of 80 °C during 50 min.

Experimental methodology

Below are the key aspects of the experimental program conducted to characterize the adhesive bonding of the composite material against delamination under modes I and II fracture stress. Both static and fatigue tests were carried out on specimens aged for different periods of exposure to a saline environment.

Surface treatment

The composite material used as the substrate was surface-conditioned by manually sanding with Al_2O_3 sandpaper with a grit size of P220. After treating the surface of the composite, it was cleaned and degreased, and then the bonding process was carried out.

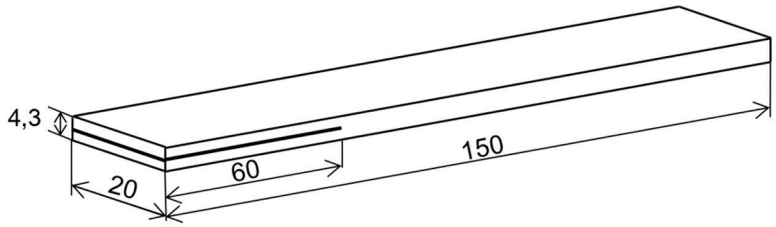

Fig. 1. Schema of specimen geometry.

Table 1
Mechanical properties of substrate.

Material	Elastic modulus[a]		Tensile strength[a]		Shear modulus[b]	Shear strength[b]
	E_{11} (GPa)	E_{22} (GPa)	σ_{11} (MPa)	σ_{22} (MPa)	G_{12} (GPa)	$\tau_{máx}$ (MPa)
MTC510-UD300-HS	122 CV = 8,5 %	8,5 CV = 8 %	1156 CV = 12,5 %	28 CV = 11,8 %	5,2 CV = 9,8 %	37 CV = 2 %

[a] ASTM D3039/D3039M-08 (ASTM D3039/D3039M-08 2008).
[b] ASTM D3518/D3518M-18 (ASTM D3518/D3518M-18 2018).

Table 2
Mechanical properties of the adhesive.

	Base	Viscosity [mPa·s] (cP)	Elastic modulus [GPa]	Tensile strength [MPa]	Shear strength [MPa]
Loctite® EA 9461TM	Epoxy	150,000 a 250,000	2.758	30.3	13.8

Saline environment degradation

In order to accelerate the aging process in a saline environment, according with ASTM B117-11 (2011), a Köheler salt spray chamber, model DCTC 1200 P, was used. The considered average temperature inside the chamber ~~of~~ was 35 °C ± 2 °C. The saline solution was prepared by dissolving 5 parts by mass of sodium chloride, with less than 0.3 % of total impurities, in 95 parts of demineralized distilled water This solution has a relative density between 1.0255 and 1.0400 g/cm^3 and a pH between 6.5 and 7.2. A relative humidity of 89 % and an air pressure of 1.2 bars were chosen because they are values close to atmospheric reality.

At the end of the process, the specimens were removed from the chamber, cleaning the residues of the saline solution. The selected exposure times in the salt spray chamber were 1 and 12 weeks under the conditions above.

Characterization of material behavior against delamination

Mode I

The ERR of mode I fracture has been utilized to analyze the influence of the aging process on the delamination phenomenon, under static and fatigue conditions. Five Double-Cantilever-Beam static tests were conducted for each aging period, determining the force levels required for delamination initiation. These values were used as a reference for planning dynamic tests. These dynamic tests were conducted at various displacement levels, ranging from 60 % to 20 % of the values obtained in the static tests.

The geometry of specimens was detailed at the begining of section 2. The specimen was placed on the testing tools so that the pre-crack tip reached 50 mm from the load line.

The tests methodology was according ASTM D5528/D5528M-21 (2021), using piano hinges for load application, as shown in Fig. 2 below.

From the formulations outlined in this standard, and considering the slight deviations presented by the three fundamental formulations proposed therein, the Modified Beam Theory (MBT) was selected as the reference for determining the ERR under mode I fracture stress. Therefore, G_{IC} was calculated using the following equation, to assess fatigue behavior:

$$G_{Ic} = \frac{3P\delta}{(2b(a+|\Delta|))} \quad (1)$$

Where b is the width of the specimen, P is the applied load, δ is the displacement at the point of load application, a is the delamination length of the crack, and Δ is a correction factor obtained based on flexibility and crack length.

Mode II

For mode II, static and fatigue End-Notched-Flexure tests (ENF) were carried out, according to ASTM D7905/D7905M-19e1 (ASTM D7905/D7905M-19e1 2019).

The geometry of the specimens was the same that for mode I, detailed at the begining of section 2. The specimen was placed on the testing tools so that the pre-crack tip reached 25 mm from the support as shown in Fig. 3 below.

The determination of the rate of fracture energy release in mode II (G_{IIC}) involved employing the experimental calibration of flexibility (NPC), the formula for which is provided in the following equation:

$$G_{IIC} = \frac{3m\,P_{MAX}^2\,a_0^2}{2B} \quad (2)$$

Where B is the specimen width, P_{MAX} is the maximum applied load, a_0 is the initial crack and m is a parameter determined by the compliance of the specimen.

For both fracture modes, mode I and mode II, an MTS-810 servo-hydraulic testing machine equipped with a 1 kN load cell was utilized.

Fig. 2. Specimen arrangement on the testing machine for mode I tests.

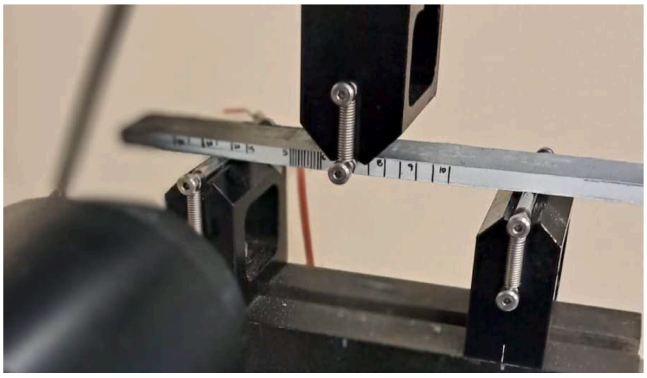

Fig. 3. Specimen arrangement on the testing machine for mode II tests.

Crack propagation was monitored using a high-resolution camera..

Fatigue characterization

In order to analyze the potential influence of exposure to a saline environment on the selected adhesive joint, its behavior regarding fracture delamination in modes I and II, and fatigue loading is studied. This includes both the fatigue delamination initiation phase and the subsequent crack growth phase.

The number of cycles required for delamination initiation with a specific ERR, is used to plot the variability of ERR vs. number of cycles curves (ΔG-N). The delamination energy level is defined based on values obtained from prior static characterization. Various levels of ERR are selected, with a coefficient of asymmetry of $R = 0.1$. Crack initiation is identified through direct observation of the specimen, establishing the initiation cycle count as the number of load cycles elapsed from the beginning of the test until a visible crack appears. Testing follows ASTM D 6115–97 (2019), recommendations at six constant force levels based on values from prior static characterization for each exposure period, combined with isolated tests to enhance result reliability. All fatigue tests are conducted under displacement control on the testing equipment, at a frequency of 3 Hz.

The standard only include the crack initiation point. To determinate the crack growth rate, periodic recordings of load, displacement, and delamination length are registered. Therefore, at intervals of every thousand cycles, the test is paused, returning to mid displacement level for measurement of the crack length. This facilitates the calculation of the ERR average applied during those cycles and the crack growth rate. Consequently, the growth rate for various crack lengths is identified, with measurements taken on the specimen surface utilizing a high-resolution camera.

For studying crack growth under mode I, the methodology proposed by Stelzer et al. (2012) is followed, where load and displacement values are defined based on prior static characterization.

For mode II, crack growth velocity is determined for different G_{IIC} percentages, requiring measurement of crack length evolution using a 100x microscope mounted on a device with controlled displacements via micrometers. Although conducting the test under these conditions is difficult and laborious, it is considered a sufficiently reliable methodology, with the provided information being valid even considering differences in crack growth across the specimen width. Similar to crack initiation tests, asymmetry coefficients ($R = 0.2$) are used.

Experimental results and discussion

Static

In Table 3, the experimental results obtained under quasi-static loading conditions of the studied adhesive joint are presented as the average of five tested specimens for each aging level. The critical ERR calculated for each fracture mode is indicated for the different exposure periods in the salt spray chamber.

Table 3
Mode I and II fracture behavior as a function of exposure time in the salt spray chamber.

Aging time	Mode I G_{IC} [J/m^2] (MBT)	Mode II G_{IIC} [J/m^2] (NPC)
No exposure	641	2096
1 week	710	2226
12 weeks	575	1918

The results presented in Table 2 are obtained as the average of 5 specimens for each exposure period and fracture mode in static tests. These values will be used later as reference in the setup of dynamic tests.

According to the results, a consistent trend is evident for both fracture modes. It is noteworthy that the best values of ERR were obtained with a exposure period of one week, which are approximately 10.7 % higher for mode I and 6.2 % higher for mode II compared to the reference values without exposure. Conversely, exposure periods of 12 weeks lead to a decrease in ERR of approximately 10.3 % for mode I and 8.5 % for mode II.

Fatigue

Initiation of the fatigue delamination process

In order to enhance the reliability in evaluating the results obtained in the experimental program, a probabilistic analysis of the entire fatigue life field was conducted, for which there are different models (El Amraoui et al., 2014; Barbosa et al., 2019; Apetre et al., 2015). In this work, a Weibull regression model proposed by Castillo et al. (Castillo and Fernández-Canteli, 2001; Castillo et al., 2008) was utilized as a statistical tool, which enables the normalization of the entire fatigue life field and has already proven effective in other cases involving composite materials (Argüelles et al., 2013).

Figs. 4, 5, and 6 show the experimental results at different levels of $G_{II\ max}$ and $G_{I\ max}$, as well as the initiation curves obtained with the Weibull model for a 5 % probability of failure. Each figure corresponds to a different exposure period (0, 1, and 12 weeks). To enhance the reliability of the probabilistic curve, it was decided to conduct at least three tests at six G levels.

To determine the crack initiation moment, continuous tracking of the crack tip is carried out using a traveling microscope. This moment is defined as the point at which a crack growth of 3 mm is reached.

For the unexposed specimens, the fatigue life range under mode II fracture varies between 1257 J/m^2 and 415 J/m^2, encompassing both low and high cycle numbers (fatigue limit), representing 60 % and 19.8 % of its static capacity, respectively. Under mode I, the fatigue life range varies between 384 J/m^2 and 160 J/m^2, representing 60 % and 25 % (fatigue limit), respectively, of its static capacity. This translates to a better response of the adhesive joint under mode I fracture in the high cycle number region and a similar trend in the low cycle number region.

For a one-week exposure in the salt spray chamber, the results achieved for mode II fracture under fatigue loading were 48.5 % and 21.5 % of its static capacity in the low and high cycle number regions, respectively. In the same regions under mode I fracture, the achieved results were 65 % and 30 %, indicating better performance of the exposed material in the high cycle number region compared to that observed for the unaged material.

For twelve weeks of exposure, the fatigue life range for mode II varies between 60 % and 18.2 % of its static capacity, while for mode I is between 64.8 % and 25 %. The trend when considering the fracture mode as an analysis parameter is the same as in the previous two cases.

For mode I, then the maximum applied ERR is taken as the test variable, a comparable trend can be observed in the high cycle number region for both the non-aged material and the material aged for one

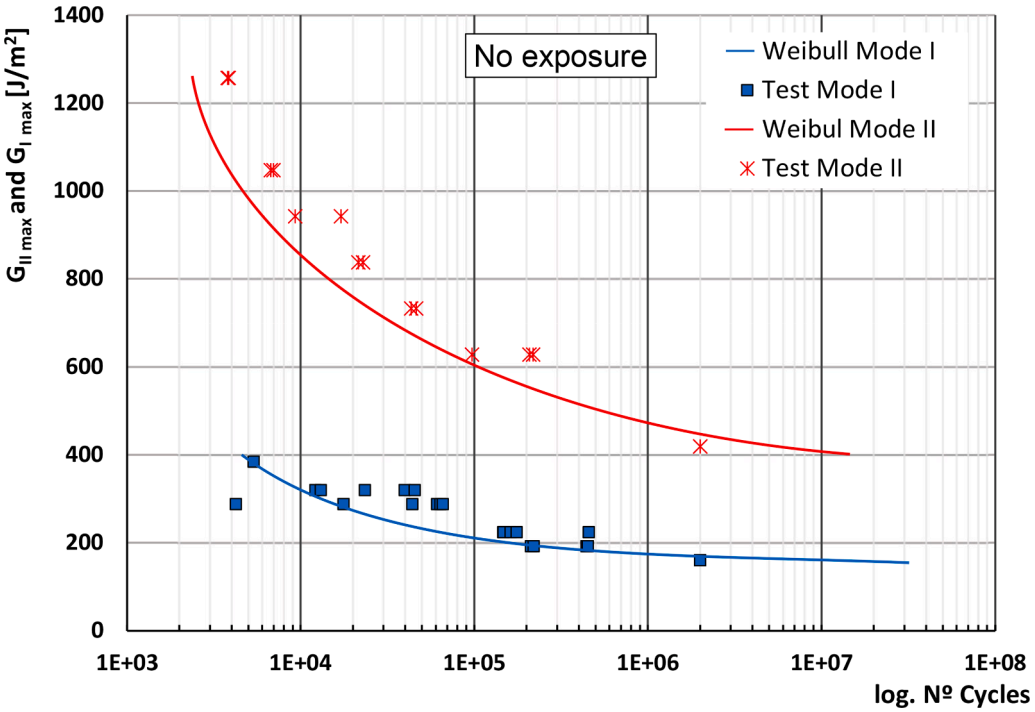

Fig. 4. Fatigue initiation curves for a 5 % failure probability in unaged material.

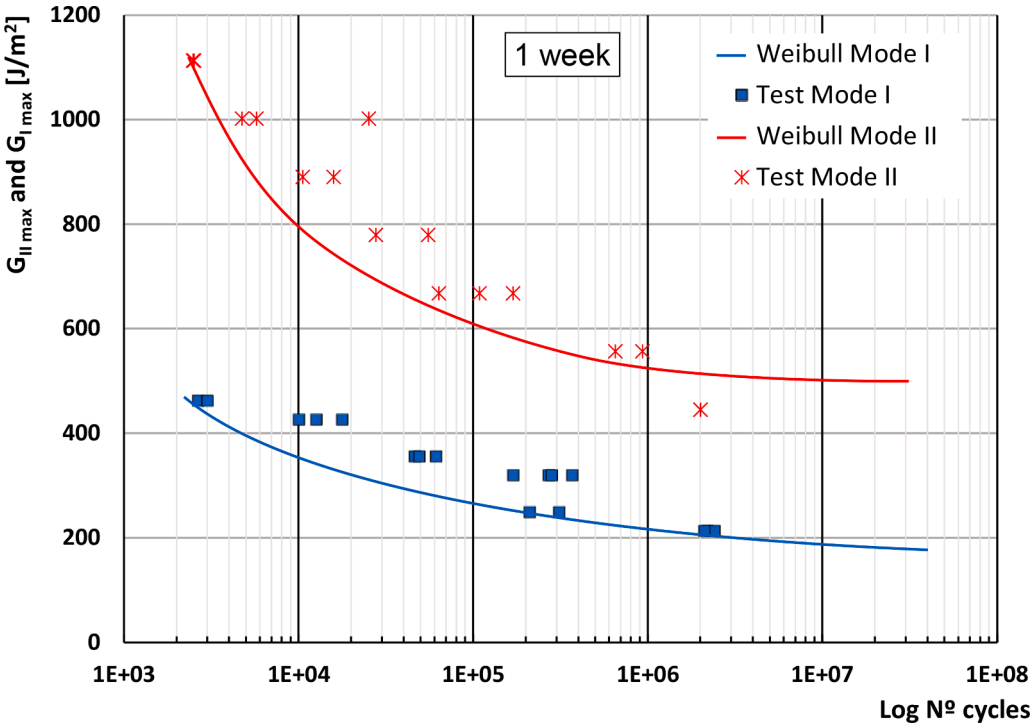

Fig. 5. Fatigue initiation curves for a 5 % failure probability, with one-week aging.

week, reaching similar fatigue limits, with a difference of approximately 5 %. If the non-aged material is compared with the material aged for 12 weeks, the difference increases to 8.7 %.

In the low cycle number region, there are differences, although not significant, tending to similar behaviors as those obtained in the previous static characterization of the material, with the same trend for the non-aged and the twelve-weeks aged materials. Slightly higher values are noted for the case of one week of aging in the salt spray chamber.

For mode II fracture solicitation in the high cycle number region, it is observed that the material shows worse fatigue behavior for twelve-weeks aging, with a fatigue limit of about 348 J/m^2 compared to 415 J/m^2 fatigue limit reached by the unexposed material. For the one-week aged material, the fatigue limit reached is about 490 J/m^2, 15% higher than that reached by the unexposed material.

Fig. 7 shows the fatigue curves of the adhesive joints studied for all the analyzed processes, illustrating the stress level expressed as a

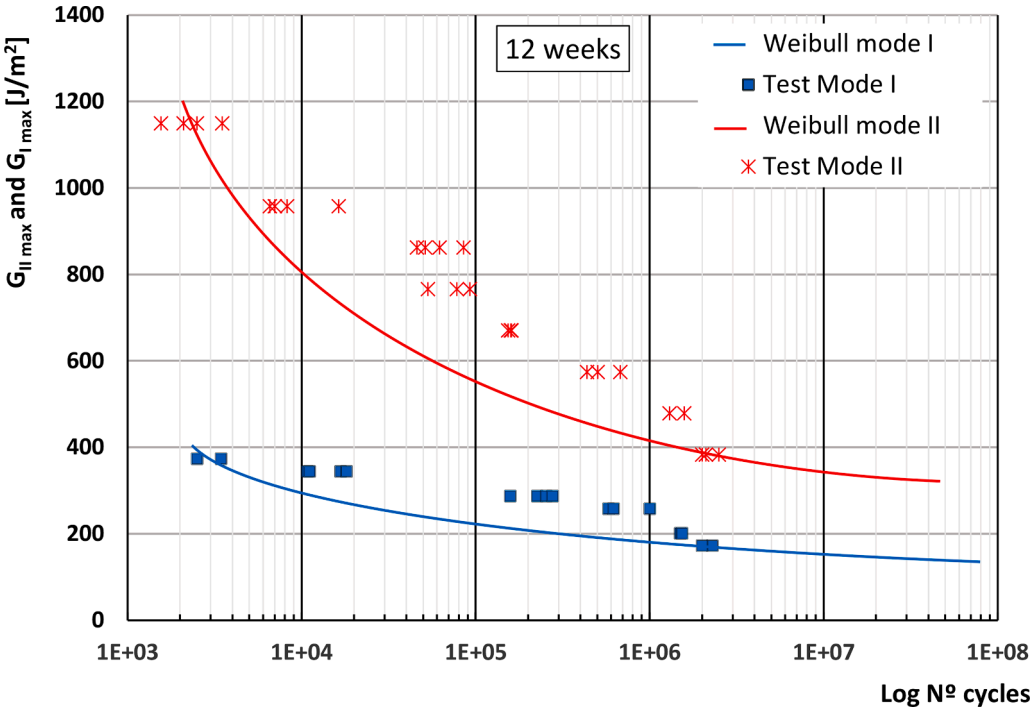

Fig. 6. Fatigue initiation curves for a 5 % failure probability, with twelve-week aging.

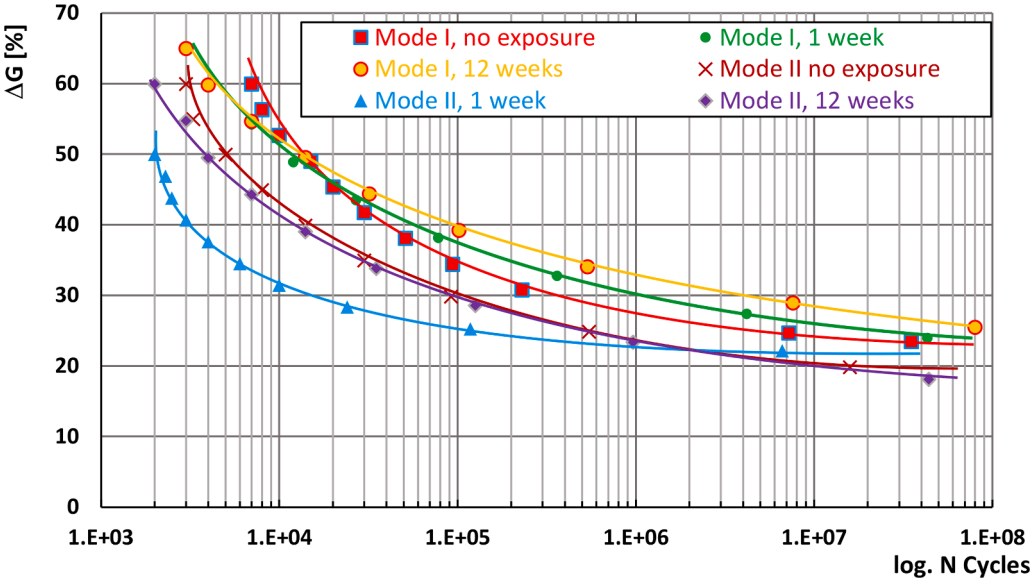

Fig. 7. Fatigue behavior for the three periods studied, for mode I and mode II.

percentage of the critical ERR obtained in the static characterization of the material versus the number of cycles endured during the fatigue test.

The behavior of adhesive joints during the fatigue delamination initiation process remains consistent across the various exposure periods studied. Both the joints without aging and those exposed to a saline environment for different durations exhibit similar fatigue curves. When considering the fatigue limit reached as the most representative parameter of behavior, and using the applied stress level as the test variable, expressed as a percentage of its ERR achieved under static loading, a consistent trend is observed regardless of the fracture mode applied (mode I or mode II). For example, in mode I, the average limit reached was 26.83 %, while in mode II, it was 19.8 % of the critical ERR of the static level.

As a summary, Table 3 presents the stress levels reached in the fatigue study conducted, expressed as a percentage of its capacity against delamination under static loading, for the material without exposure and with 1 and 12 weeks of exposure to the selected saline environment. It provides, for each of the analyzed fracture modes (mode I and mode II), the percentage achieved in both the low and high cycle regions.

To summarize the ΔG levels reached in the fatigue study, expressed as a percentage of their static delamination capacity, Table 4 shows the data for the material without exposure and with 1 and 12 weeks of exposure to the selected saline environment. The percentages achieved in both the low and high cycle regions for each analyzed fracture mode (mode I and mode II) are shown.

Based on these results, it is evident that the studied adhesive joint

Table 4
ΔG levels reached.

Aging time	Mode II [%] zone		Mode I [%] zone	
	Low number of cycles	High number of cycles	Low number of cycles	High number of cycles
No exposure	60	19,8	60	25
1 week	48,5	21,5	65	30
12 weeks	60	18,2	64,8	25,3

exhibits worse behavior in response to delamination under mode II fracture, compared to its behavior under mode I fracture.

Fatigue delamination growth

In Fig. 8, the crack growth rate under fatigue loading is plotted against the maximum normalized total ERR applied in dynamic tests relative to the critical total obtained during the previous static characterization of the studied adhesive (fracture modes I and II). The behavior of the material of representative specimens subjected to different exposure periods to the saline environment (no exposure, 1 week, and 12 weeks) is shown.

From the experimental data, for mode I, a consistent trend is inferred for the exposure periods of one and twelve weeks in the salt spray chamber, showing similar fatigue delamination growth rates and matching normalized ERRs. Overall, these rates are higher than those observed in the non-exposed material across the entire crack growth range, indicating that exposure to the saline environment leads to faster crack growth compared to non-exposed material, irrespective of the exposure duration of one or twelve weeks.

From the experimental data, it is evident that for mode I, both the one-week and twelve-week exposure periods in the salt spray chamber exhibit similar fatigue delamination growth rates and normalized ERRs. These rates are generally higher than those observed in the unexposed material across the entire crack growth field. This suggests that exposure to a saline environment leads to faster crack growth, regardless of the exposure duration.

However, for mode II, the behavior differs. While the unexposed material and the material exposed for one week exhibit similar trends, delamination growth rates are generally higher in mode II, resulting in unstable and relatively rapid delamination growth once initiated.

Fig. 9 shows the crack growth rate versus the maximum ERR applied to the bond during fatigue crack growth for both failure modes, comparing the behavior of the bond without exposure and after one and twelve weeks of exposure to the saline environment.

For mode I, it is observed that delamination growth is faster with increasing exposure time to the saline environment, although it is less favorable after one week of exposure.

In mode II, two distinct zones are observed based on the exposure duration: in the low-stress zone, the behavior is similar between the unexposed material and the material exposed for one week, while the material exposed for twelve weeks performs better, requiring a higher stress level for identical growth rates. However, in the medium and high-stress zones, the behavior differs, with the unexposed material and the material exposed for twelve weeks exhibiting similar trends, while the material exposed for one week performs better, showing lower growth rates for the same stress level.

In Fig. 10, the delamination growth rate is plotted against crack length for both pure fracture modes considered, mode I and mode II, for the material without exposure to a saline environment and with exposure periods of one and twelve weeks.

In light of the presented results, when considering fracture mode as the reference parameter in the analysis of delamination growth rate as a function of crack length, it is observed that for mode I, the crack growth rate tends to decrease when the delamination length progresses. Whereas for mode II, the growth rate remains nearly constant throughout the process. Additionally, relatively lower growth rates are observed for mode II fracture during the one-week exposure period, although the differences are minor.

Fracture surface

In order to more effectively analyze the influence of different exposure periods on the behavior of the adhesive joint when subjected to fatigue under modes I and II fracture, the resulting fracture surfaces were studied using a scanning electron microscope (SEM), model JEOL-JSM5600.

The samples used were extracted from the area closest to the crack front (insert), as indicated in Fig. 11, where the fatigue process begins. In this figure, images considered representative are showed. The study was conducted on images of different samples, witha magnification level of

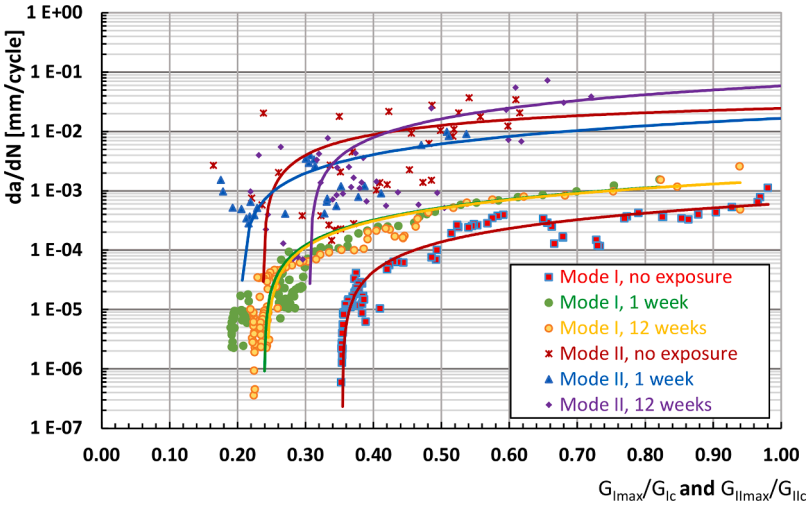

Fig. 8. Crack growth rate under fatigue versus the maximum normalized ERR for the different studied exposure periods.

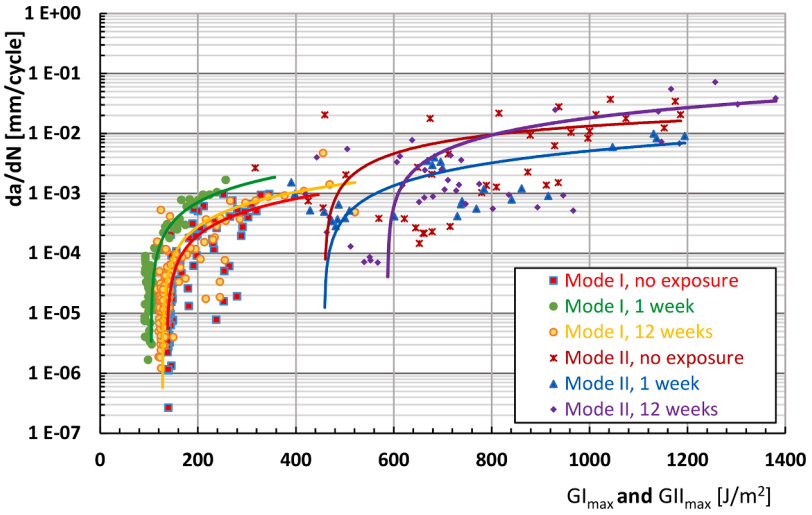

Fig. 9. Fatigue crack growth rate versus maximum applied ERR for the different exposure periods.

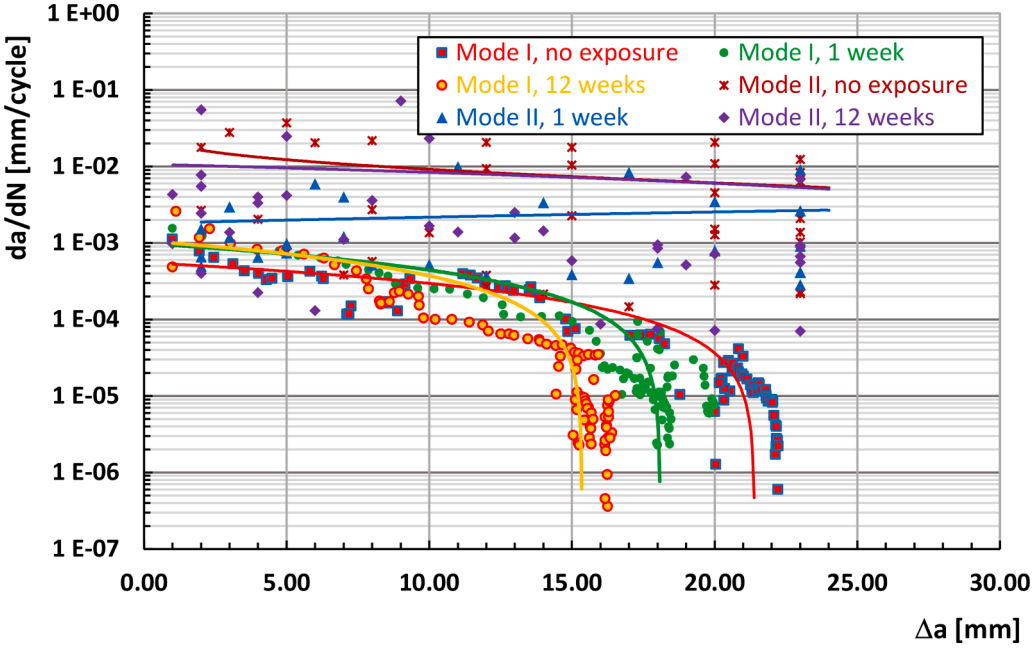

Fig. 10. Fatigue crack growth rate versus delamination length for the different exposure periods and both fracture modes I and II.

x300 in all cases.

For mode I, there is a sharp adhesive rupture with fiber tearing and a rough surface that becomes smoother with longer exposure, as can be seen in Fig. 11.c after 12 weeks. In contrast, for mode II, there's a transition from adhesive plasticity in Fig. 11.d (no exposure) to minimized plasticity in Fig. 11.e (one week exposure), disappearing entirely in Fig. 11.f after 12 weeks of exposure.

Differences in fracture surfaces were evident depending on the fracture mode applied, although for both fracture modes, a cohesive fracture is observed. It is also noticeable that the lines generated by the crack propagation are more spaced in the unaged sample and are more easily visible. This indicates a greater resistance to crack advancement due to the non-aged of the adhesive. However, in cases where aging exists, degradation of the adhesive is observed, affecting the sharpness of the crack front, resulting in smoother surfaces and material with smaller grain sizes.

Conclusions

This experimental study aimed to explore the correlation between the initiation and propagation of fatigue-induced delamination under pure fracture modes I and II in epoxy-based adhesive joints on laminates with an epoxy matrix reinforced by unidirectional carbon fibers, subject to varying durations in a high-saline environment.

Regarding the initiation of interlaminar cracks under static loading for both fracture modes and the influence of exposure time to the saline environment, it is evident that the adhesive joint performs better for short exposure periods, such as one week, where higher ERRs are achieved compared to unexposed material. However, for longer exposure periods, the achieved values are lower than those of unexposed material. This phenomenon is observed for both pure fracture modes I and II studied, indicating that the first few days of exposure lead to adhesive post-curing, improving its properties.

In dynamic loading, for initiation when considering the fatigue behavior represented by the fatigue limit, a better delamination

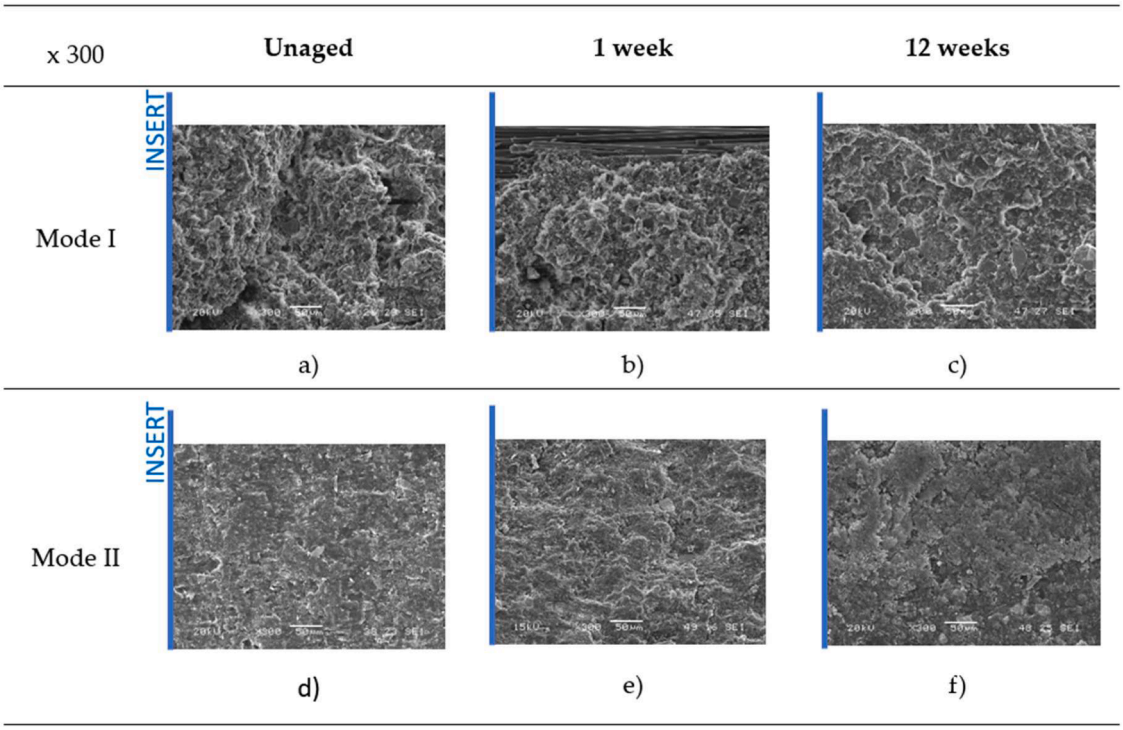

Fig. 11. Fracture surfaces of adhesive joints subjected to fatigue (modes I and II) for different periods of exposure to a saline environment. Images taken at 300x magnification.

resistance of the studied adhesive is observed under mode I fracture solicitation, regardless of the exposure period to the saline environment. The behavior of the material in the low cycle zone follows the same trend observed in the high cycle or infinite life zone.

The fatigue curves obtained in the initiation phase of the delamination process indicate a similar behavior of the adhesive joint for all cases: no exposure, one week, and twelve weeks, and for both fracture modes, with average fatigue limits of 19% for mode II and 27% for mode I, as a percentage of its static strength.

In dynamic loading, for mode I, exposure to a saline environment causes crack growth at higher rates than those observed in unexposed material, regardless of the exposure period of one or twelve weeks. For mode II a similar trend can be considered for unexposed material and material exposed to one week of salt spray chamber. In general, delamination growth rates are higher under mode II fracture, with an unstable and relatively fast delamination growth once the process is initiated.

Analyzing the delamination growth rate as a function of crack length, it is observed that for mode I, the crack growth rate tends to decrease as the delamination length increases. For mode II, the growth rate remains almost constant for any delamination length, with relatively lower growth rates for the one-week exposure period, although the differences are minor.

Significant differences are deduced from the obtained fracture surfaces between the two fracture modes and the deterioration caused in the adhesive joint by the degradation process in the salt spray chamber. In mode I, this degradation results in a change in the relief of the fracture surface, being more uneven in the unexposed material. For mode II, there is a noticeable smoothing of the fracture surface due to movement, which appears as a certain plasticization, and tends to disappear as the exposure time increases. In both modes, crack propagation is observed in the unexposed material, becoming less clear as the exposure period and the progressive deterioration of the adhesive increase, becoming imperceptible after 12 weeks of exposure.

CRediT authorship contribution statement

P. Vigón: Investigation. **A. Argüelles:** Validation. **M. Lozano:** Methodology. **J. Viña:** Supervision.

Declaration of competing interest

The authors declare that they have no known competing financial interests or personal relationships that could have appeared to influence the work reported in this paper.

Data availability

Data will be made available on request.

Acknowledgements

The authors would like to thank the Vice-Rectorate for Research at the University of Oviedo, through the Research Support and Promotion Plan, for their financial support through the project PAPI-22-PF-16

References

Abdel-Monsef, S., Renart, J., Carreras, L., Turon, A., Maimí, P., 2021. Effect of environment conditioning on mode II fracture behaviour of adhesively bonded joints. Theor. Appl. Fracture Mech. 112, 102912 https://doi.org/10.1016/j.tafmec.2021.102912.

Akhavan-Safar, A., Sh, Jalali, da Silva, L.F.M., Ayatollahi, M.R., 2023. Effects of low cycle impact fatigue on the residual mode II fracture energy of adhesively bonded joints. Int. J. Adhes. Adhes. 126, 103455 https://doi.org/10.1016/j.ijadhadh.2023.103455.

Almansour, F.A., Dhakal, H.N., Zhang, Z.Y, 2017. Effect of water absorption on Mode I interlaminar fracture toughness of flax/basalt reinforced vinylester hybrid composites. Compos. Struct. 168, 813–825. https://doi.org/10.1016/j.compstruct.2017.02.081.

Apetre, N., Arcari, A., Dowling, N., Iyyer, N., Phan, N., 2015. Probabilistic model of mean stress effects in strain-life fatigue. Procedia Eng. 114, 538–545. https://doi.org/10.1016/j.proeng.2015.08.103.

Argüelles, A., Coronado, P., F, Canteli, A., Viña, J., Bonhomme, J, 2013. Using a statistical model for the analysis of the influence of the type of matrix carbon-epoxy composites on the fatigue delamination under modes I and II of fracture. Int. J. Fatigue 56, 54–59. https://doi.org/10.1016/j.ijfatigue.2013.08.001.

Argüelles, A., Viña, I., Vigón, P., Lozano, M., Viña, J., 2022. Study of the fatigue delamination behaviour of adhesive joints in carbon fibre reinforced epoxy composites, influence of the period of exposure to saline environment. Sci. Rep. 12, 19789. https://doi.org/10.1038/s41598-022-23378-4.

ASTM B117-11, 2011. Standard Practice for Operating Salt Spray (Fog) Apparatus. ASTM International, West Conshohocken, PA, USA.

ASTM D 6115-97, 2019. Mode I fatigue Delamination Growth Onset of Unidirectional Fiber-Reinforced Polymer Matrix Composites, 2019. ASTM International, West Conshohocken, PA, USA.

ASTM D3039/D3039M-08, 2008. Standard Test Method For Tensile Properties of Polymer Matrix Composite Materials. ASTM International, West Conshohocken, PA, USA.

ASTM D3518/D3518M-18, 2018. Standard Test Method For In-Plane Shear Response of Polymer Matrix Composite Materials By Tensile Test of a ±45° Laminate. ASTM International, West Conshohocken, PA, USA.

ASTM D5528/D5528M-21, 2021. Standard Test Method For Mode I interlaminar Fracture Toughness of Unidirectional Fiber-Reinforced Polymer Matrix Composites. ASTM International, West Conshohocken, PA, USA.

ASTM D7905/D7905M-19e1, 2019. Standard Test Method For Determination of the Mode II Interlaminar Fracture Toughness of Uni-directional Fiber-Reinforced Polymer. ASTM International, West Conshohocken, PA, USA.

Barbosa, J.F., Correia, J A F O, Júnior R C S, Freire, Zhu, S.-P., de Jesus, AMP., 2019. Probabilistic S-N fields based on statistical distributions applied to metallic and composite materials: state of the art. Adv. Mech. Eng. 11 (8), 1–22. https://doi.org/10.1177/1687814019870395.

Brito, C.B.G., Sales, R.C.M., Donadon, M.V., 2020. Effects of temperature and moisture on the fracture behaviour of composite adhesive joints. Int. J. Adhes. Adhes. 100, 102607 https://doi.org/10.1016/j.ijadhadh.2020.102607.

Brunner, A.J., Warnetb, L., Blackman, B.R.K., 2021. 35 years of standardization and research on fracture of polymers, polymer composites and adhesives in ESIS TC4: past achievements and future directions. Procedia Struct. Integr. 33, 443–455. https://doi.org/10.1016/j.prostr.2021.10.051.

Castillo, E., Fernández-Canteli, A., 2001. A general regression model for lifetime evaluation and prediction. Int. J. Fatigue 107, 117–137. https://doi.org/10.1023/A:1007624803955.

Castillo, E., Fernández-Canteli, A., Pinto, H., López-Aenlle, M., 2008. A general regression model for statistical analysis of strain life fatigue data. Mater. Lett. 62, 3639–3642. https://doi.org/10.1016/j.matlet.2008.04.015.

Clerca, G., Brunner, A.J., Josset, S., Niemz, P., Pichelin, F., Van de Kuilend, J.W.G., 2019. Adhesive wood joints under quasi-static and cyclic fatigue fracture Mode II loads. Int. J. Fatigue 123, 40–52. https://doi.org/10.1016/j.ijfatigue.2019.02.008.

Del Real, J.C., Ballesteros, Y., Chamochin, Y., Abenojar, J., Molisani, L., 2011. Influence of surface preparation on the fracture behavior of acrylic adhesive/CFRP composite joints. J. Adhes. 87 (4), 366–381. https://doi.org/10.1080/00218464.2011.562114.

Delzendehroo, F., Beygi, R., Akhavan-Safar, A., da Silva, L.F.M., 2021. Fracture energy assessment of adhesives Part II: is GIIc an adhesive material property? (A neural network analysis). J. Adv. Join. Process. 3, 100049 https://doi.org/10.1016/j.jajp.2021.100049.

Desai, C.R., Patel, D.C., K;, Chaitaniya K.Desai C, 2023. Investigations of joint strength & fracture parameter of adhesive joint: a review. In: Materials Today: Proceedings. https://doi.org/10.1016/j.matpr.2023.04.026.

El Amraoui, A., El Gharad, A., Bensalah, M.O., 2014. On stochastic evaluation of S - N models based on lifetime distribution. Appl. Math. Sci. 8, 1323–1331. https://doi.org/10.12988/ams.2014.412.

Fernandes, R.L., de Moura M F S, F., Moreira, R.D.F., 2016. Effect of temperature on pure modes I and II fracture behavior of composite bonded joints. Compos. Part B: Eng. 96, 35–44. https://doi.org/10.1016/j.compositesb.2016.04.022.

González Ramírez, F.M., Parise Garpelli, F., Mendonça Sales, R de C, Cândido, G.M., Arbelo, M.A., Yutaka Shiino, M., Donadon, M.V, 2018. Experimental characterization of Mode I fatigue delamination growth onset in composite joints: a comparative study. Mater. Design 160, 906–914. https://doi.org/10.1016/j.matdes.2018.10.007.

Johar, M., Chong, W.W.F., Kang, H.S., Wong, K.J., 2019. Effects of moisture absorption on the different modes of carbon/epoxy composites delamination. Polym. Degrad. Stab. 165, 117–125. https://doi.org/10.1016/j.polymdegradstab.2019.05.007.

Katafiasz, T.J., Greenhalgh, E.S., Allegri, G., Pinho, S.T., Robinson, P, 2021. The influence of temperature and moisture on the mode I fracture toughness and associated fracture morphology of a highly toughened aerospace CFRP. Compos. Part A Appl. Sci. Manuf. 142, 106241 https://doi.org/10.1016/j.compositesa.2020.106241.

Lima, R.A.A., Migliavacca, F., Martulli, L.M., Carboni, M., Bernasconi, A, 2022. Distributed fibre optic monitoring of mode I fatigue crack propagation in adhesive bonded joints and comparison with digital image correlation. Theor. Appl. Fracture Mech. 121, 103501 https://doi.org/10.1016/j.tafmec.2022.103501.

Martínez-Landeros, V.H., Vargas-Islas, S.Y., Cruz-González, C.E., Barrerad, S., Mourtazov, K., Ramírez-Bon, R, 2019. Studies on the influence of surface treatment type, in the effectiveness of structural adhesive bonding, for carbon fiber reinforced composites. J. Manuf. Process. 39, 160–166. https://doi.org/10.1016/j.jmapro.2019.02.014.

Mohan, J., Ivankovic, A., Murphy, N., 2014. Mode I fracture toughness of co-cured and secondary bonded composite joints. Int. J. Adhes. Adhes. 51, 13–22. https://doi.org/10.1016/j.ijadhadh.2014.02.008.

Orell, O., Jokinen, J., Kanerva, M., 2023. Use of DIC in the characterisation of mode II crack propagation in adhesive fatigue testing. Int. J. Adhes. Adhes. 122, 103332 https://doi.org/10.1016/j.ijadhadh.2023.103332.

Saleh, M.N., Tomic, N.Z., Marinkovic, A., de Freitas, S.T, 2021. The effect of modified tannic acid (TA) eco-epoxy adhesives on mode I fracture toughness of bonded joints. Polym. Test. 96, 107122 https://doi.org/10.1016/j.polymertesting.2021.107122.

Santos, D., Akhavan-Safar, A., Carbas, R.J.C., Marques, E.A.S., Wenig, S., da Silva, L.F.M., 2023. Load-control vs. displacement-control strategy in fatigue threshold analysis of adhesives: effects of temperature. Eng. Fract. Mech. 284, 109255 https://doi.org/10.1016/j.engfracmech.2023.109255.

Sousa, F.C., Akhavan-Safar, A., Carbas, R.J.C., Marques, E.A.S., Barbosa, A.Q., da Silva, L.F.M., 2023. Experimental study on the influence of environmental conditions on the fatigue behaviour of adhesive joints. Int. J. Fatigue 175, 107752. https://doi.org/10.1016/j.ijfatigue.2023.107752.

Stelzer, S., Brunner, A.J., Argüelles, A., Murphy, N., Pinter, G., 2012. Mode I delamination fatigue crack growth in unidirectional fiber reinforced composites: development of a standardized test procedure. Compos. Sci. Technol. 72, 1102–1107. https://doi.org/10.1016/j.compscitech.2011.11.033.

Tan, W., Na, J., Wang, G., Xu, Q., Shen, H., Mu, W., 2021. The effects of service temperature on the fatigue behavior of a polyurethane adhesive joint. Int. J. Adhes. Adhes. 107, 102819 https://doi.org/10.1016/j.ijadhadh.2021.102819.

Teixeira de Freitas, S., Banea, M.D., Budhe, S., de Barros, S., 2017. Interface adhesion assessment of composite-to-metal bonded joints under salt spray conditions using peel tests. Compos. Struct. 164, 68–75. https://doi.org/10.1016/j.compstruct.2016.12.058.

Vigón, P., Argüelles, A., Mollón, V., Lozano, M., Bonhomme, J., Viña, J., 2022. Study of the influence of the type of aging on the behavior of delamination of adhesive joints in carbon-fiber-reinforced epoxy composites. Materials (Basel) 15, 3669. https://doi.org/10.3390/ma15103669.

Vikas, K., Bar, H.N., Ghosh, A, 2021. Influence of extremely cold environmental conditions on interfacial fracture phenomenon of aerospace grade unidirectional composites. Thin-Walled Struct. 161, 107431 https://doi.org/10.1016/j.tws.2020.107431.

Yildirim, C., Ulus, H., Beylergil, B., Al-Nadhari, A., Topal, S., Yildiz, M., 2023. Effect of atmospheric plasma treatment on Mode-I and Mode-II fracture toughness properties of adhesively bonded carbon fiber/PEKK composite joints. Eng. Fract. Mech. 289, 109463 https://doi.org/10.1016/j.engfracmech.2023.109463.

Zabala, H., Aretxabaleta, L., Castillo, G., Aurrekoetxea, J., 2016. Dynamic 4 ENF test for a strain rate dependent mode II interlaminar fracture toughness characterization of unidirectional carbon fibre epoxy composites. Polym. Test. 55, 212–218. https://doi.org/10.1016/j.polymertesting.2016.09.001.